

venient to do this using the thermal gradient. It is difficult, however, to measure the period definitively in the homogeneous case, primarily because of its sensitivity to the rate of stirring. This appears to be due to the effect of stirring on the transfer of gases (such as  $\text{Br}_2$ ,  $\text{O}_2$ ) across the free surface (8). Another complicating factor is that the period changes slowly with age in a manner that appears to depend on the temperature, gas transfer, and so forth throughout the previous evolution of the reaction. Nevertheless, on the whole, such measurements of the period at different temperatures seemed to agree with what one deduces from pictures like Fig. 2 in the thermally stratified case.

As the scale of the bands becomes finer it must be expected that eventually diffusion will begin to play a role. One can construct mathematical models which show that diffusion can counter the imposed period gradient to stop the formation of an ever-finer scale structure and lead to a situation in which the frequency is uniform (even though the basic concentration gradient remains). However, we estimated that, within our concentration ranges, this would take an amount of time on the order of the lifetime of the overall reaction (8). (It takes far longer—approximately a month—for the basic concentration gradient to diffuse away.) Hence we do not have any experimental evidence of the role of diffusion in the band patterns.

The kinematic model also predicts some other effects that are observed. For example, if there is a gradient of  $\text{H}_2\text{SO}_4$  (so that propagation is upward), the bands tend to curve downward near the walls. The kinematic mechanism says that even if the phases are a function not only of height,  $z$ , but also of some horizontal coordinate  $y$ , the fronts  $\Phi(z,x,t) = 2\pi k$  will approach the horizontal as long as the period is just a function of height. For then  $\Phi(z,x,t) = \Psi(z,t) + \Phi_0(z,x,t)$ , where  $\Psi$  is as before and  $\Phi_0$  is the initial distribution of phases. As before, the initial conditions wash out. In general, the bands tend toward the shape of the surfaces of constant period. If the only factor affecting the period is concentration and if this is tied to density, these constant-period surfaces will be horizontal. However, the period of the Belousov oscillation is also affected by temperature. Since the reaction is exothermic, the fluid near the walls of the container is somewhat cooler, and so it

oscillates more slowly. Hence the surfaces of constant period tend to curve downward near the walls. From the hydrodynamic equations it is possible to estimate the size of this effect and show it to be approximately what one observes in the downward curving of the bands (8). The exothermicity alone, without the period gradient, cannot cause the propagation of the bands or keep them horizontal (8); indeed the pulses of heat given off by the reaction cause very little fluid motion, and whatever there is tends to increase rather than decrease any perturbation of the bands from the horizontal.

Another effect partially due to kinematic mechanisms is the rapid loss of all temporal or spatial structure in the solution when it is placed in a beaker with no external gradient and not stirred. Our experiments show that in this situation the reaction is still oscillating at each point in the fluid, but at somewhat different frequencies (possibly because of temperature fluctuations), so that the phases are random. Also, in the absence of the external density gradient, temperature differences due to the heating from the reaction and cooling along the boundaries are enough to drive irregular convective motion of the fluid. Patterns formed in this situation by kinematic mechanisms are irregular because of the random fluctuations in temperature, and they are further convoluted by the convective motion. Hence, after a short time, there is no visible structure.

The horizontal bands described here are quite stable, and a visible structure remains for some time. In this case

there is, in general, a density gradient as well as a period gradient. The period gradient dominates irregular variations so that the constant-period surfaces remain nearly horizontal. The density gradient prevents convective motion. Hence, the horizontal bands due to, say, a sulfuric acid gradient may be expected to be stable. When there is no associated density gradient (for example, with a cerium gradient) the bands are much less stable.

N. KOPELL

Department of Mathematics,  
Northeastern University,  
Boston, Massachusetts 02115

L. N. HOWARD

Department of Mathematics,  
Massachusetts Institute of Technology,  
Cambridge 02139

#### References and Notes

1. B. P. Belousov, in *Sb. Ref. Radiat. Med.* (Collection of abstracts on radiation medicine) (Medgiz, Moscow, 1959), p. 145.
2. R. M. Noyes, R. J. Field, E. Körös, *J. Amer. Chem. Soc.* **94**, 1394 (1972).
3. A. M. Zhabotinskii, *Dokl. Akad. Nauk SSSR* **157**, 392 (1964); V. A. Vavilin and A. M. Zhabotinskii, *Kinet. Katal.* **10**, 83, 657 (1969); H. Degn, *Nature* **213**, 589 (1967); G. J. Kasperek and T. C. Bruice, *Inorg. Chem.* **10**, 382 (1971); R. M. Noyes, R. J. Field, R. C. Thomson, *J. Amer. Chem. Soc.* **93**, 7315 (1971).
4. J. F. Lefelhocz, *J. Chem. Educ.* **49**, 312 (1972).
5. H. G. Busse, *J. Phys. Chem.* **73**, 750 (1969).
6. A. N. Zaikin and A. M. Zhabotinskii, *Nature* **225**, 535 (1970).
7. R. J. Field and R. M. Noyes, *ibid.* **237**, 390 (1972); R. J. Field, *J. Chem. Educ.* **49**, 308 (1972); A. T. Winfree, *Science* **175**, 634 (1972).
8. L. N. Howard and N. Kopell, in preparation.
9. N. Kopell and L. N. Howard, in preparation.
10. The mixture consisted of 0.3M malonic acid, 0.08M potassium bromate, 0.002M cerous sulfate, 0.75 to 2.2M sulfuric acid, and 0.0006M ferroin. The temperature was 25°C.
11. Supported by the National Science Foundation.
12. February 1973

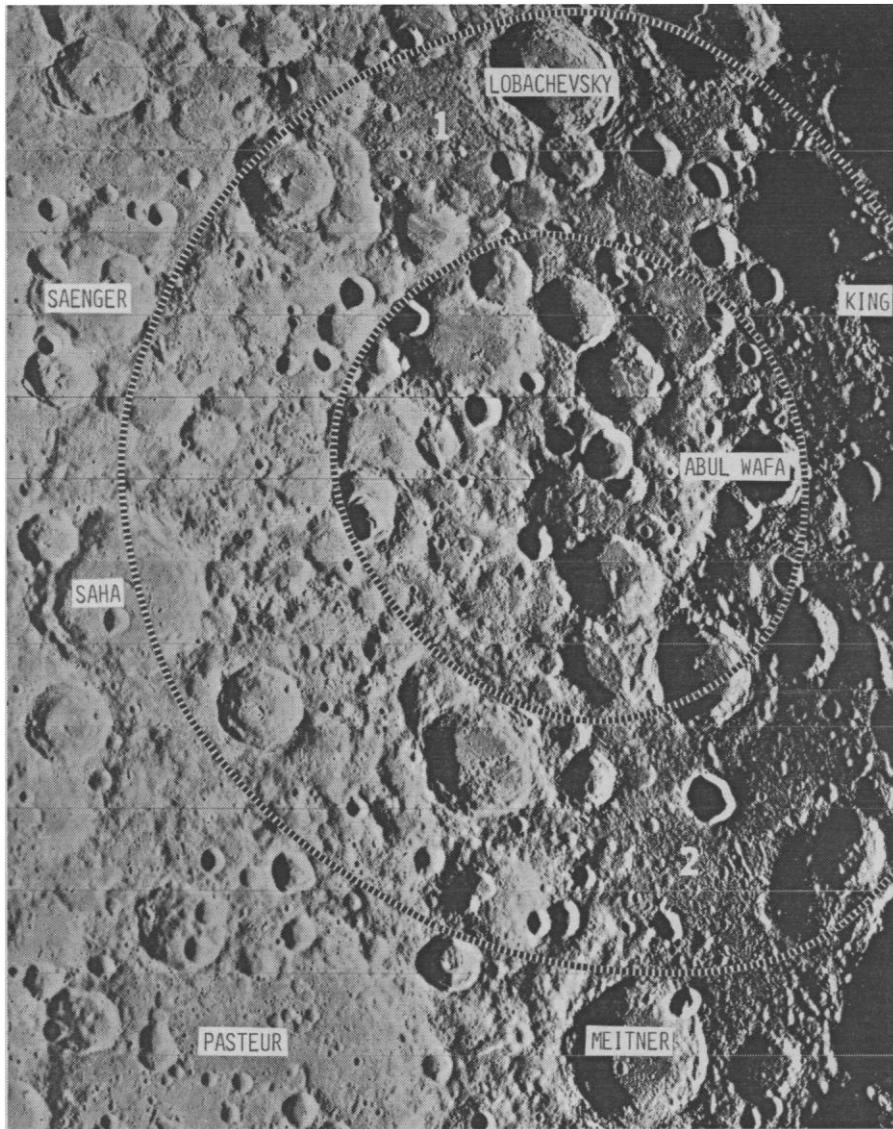
## Al-Khwarizmi: A New-Found Basin on the Lunar Far Side

**Abstract.** *Apollo 16 and Apollo 17 photographs of the far side of the moon reveal a double-ringed basin 500 kilometers in diameter centered at 1°N, 112°E. The structure is very old and subdued; it is probably Pre-Nectarian in age and appears to have been filled and modified by younger events. The heights of the basin's rings are based on laser altimeter data from Apollo missions 15 through 17; these data suggest a third outer ring, approximately 1000 kilometers in diameter. Laser measurements also indicate that the filled basin separates the relatively low terrain on the eastern limb of the moon from the higher, more rugged highlands to the east.*

In the course of planning orbital photography and visual observations on Apollo missions 15 through 17, the astronauts and I studied the interesting crater King and its environs (1). The pilots of the command modules of the three missions took photographs and made visual observations of features in

this region of the farside highlands. They described the King crater area, previously labeled the "Soviet Mountains" (2), as a plateau, a gentle rise which they compared to another rise around the crater Saenger (4.5°N, 102.5°E).

Study of the Apollo photographic



records revealed the presence in the region of a large, multiringed basin centered at  $1^{\circ}\text{N}$ ,  $112^{\circ}\text{E}$ . The aforementioned plateaus form parts of the basin's rings that are also shown in earlier Lunar Orbiter photographs (Fig. 1). However, the discovery of the basin was made possible by the more complete Apollo metric and panoramic camera records.

The basin displays two distinct rings with a third probable outer ring. Correlation of the basin's morphology with that of other lunar basins suggests that it is Pre-Nectarian in age; it is probably among the oldest basins with visible remains on the lunar surface. The sharpness of its rings decreases outward; the innermost ring (270 km in diameter) is the sharpest, and the probable third ring (1000 km in diameter) is the least obvious. The eastern and western portions of the second ring (500 km in diameter) are represented by broad plateaus with relatively sharp inward-facing scarps. This feature is also characteristic of the intermediate ring of the three-ringed Orientale basin, although they are here discontinuous and much more degraded than in the Orientale case.

The recognizable part of the eastern plateau of the second ring is about 300 km long and 120 km wide; the western plateau is up to 600 km long with a maximum width of 90 km. Figure 2 shows the relationship of the basin to other formations near the eastern limb of the moon.

An old and subdued crater 200 km in diameter was also discovered on the eastern border of the second ring (Fig. 2). This new-found crater is centered at about  $3^{\circ}\text{S}$ ,  $125^{\circ}\text{E}$ . Although probably Pre-Nectarian in age, the 200-km crater and its rim deposits exhibit superposition relationships that indicate its young age relative to that of the basin (3).

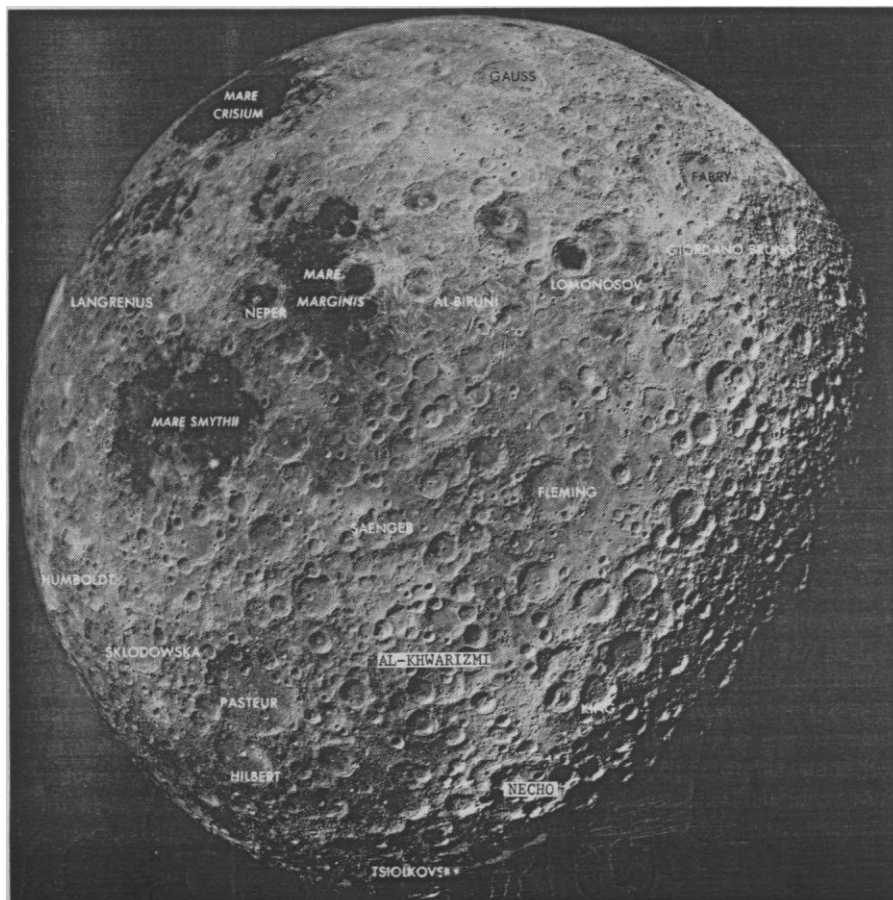


Fig. 1 (top). Part of Lunar Orbiter II frame 196-M showing two rings of the new-found basin. The interior of the basin is filled by later deposits from cratering events. Two regions occupied by plains (1, in the northern segment surrounding Lobachevsky; and 2, in the southern part, north-northeast of Meitner) are typical of the interiors of other old lunar basins. Fig. 2 (bottom). Full-disk view of the moon obtained by the mapping camera (frame 3023) following departure from lunar orbit on Apollo mission 16. The new-found Al-Khwarizmi basin is in the middle of the lower part of the disk; the newly discovered crater Necho, 200 km in diameter, is in the lower-right part of the disk.

Laser altimeter data from Apollo missions 15 through 17 provided further information on the new-found basin: Apollo 16 ground tracks crossed the middle of the basin; the Apollo 15 spacecraft flew over its southwestern part (Fig. 3a); and Apollo 17 laser data, which are not discussed here, duplicate parts of both the Apollo 16 and the Apollo 17 data.

On these missions, range measurements from the orbiting spacecraft to the lunar surface were made. The altitude was computed from altimeter slant range on the assumption that the moon is a sphere having a radius of 1738 km (4). The laser profiles provide height measurements of the basin rings relative to its filled floor.

As shown in Fig. 3b, and starting at 140°E, the Apollo 16 laser profile crosses the floor of the large crater Mendeleev which is about 6 km deep. After a 2.8-km depression representing the crater Green, there is a drop of 3.5 km, perhaps representing the third ring of the basin at 120°E. A gentle rise indicates the beginning of the second ring whose peak occurs at 122°E. Its inward-facing scarp rises about 1 km above the mean lunar radius. The eastern border of the first ring is at the crater Abul Wafa, and its western border under the orbital tracks occurs at 107°E.

Within the innermost ring and centrally located is a considerable rise that is 75 km in diameter. This rise may represent a surface expression of an uplift in the center of the excavation, possibly due to the impact which created the basin.

The inward-facing scarp of the western part of the second ring rises 2.7 km above the mean lunar radius. Following a depression that is magnified by the crater Wyld, the probable third ring is detected at 95°E. It is modified by, and possibly covered by, ejecta from Mare Smythii. At this point, however, the probable third ring of the basin (or the rim of Mare Smythii, or both) is lower than the mean lunar radius. This depression is possibly due to the fact that this is a part of the lunar crust that was considerably lower than the surroundings, that is, prior to the formation of both the new-found basin and Mare Smythii. The latter, as shown by laser altimeter data (4), is the deepest basin on the moon.

The applicable portion of the Apollo 16 laser altimeter profile starts at 125°E with a sharp drop that probably represents the scarp of the least well-

defined outermost ring (Fig. 3c). The scarp rises about 2 km above the mean lunar radius and appears to separate the basin area from the relatively higher terrain to the east. The altitude traverse encounters the second ring at two locations (113°E and 104°E). From the peak of the western scarp of the second ring (at 104°E, 2.6 km higher than the

mean lunar radius) westward, the profile closely follows that of Apollo 15.

According to the rules of the International Astronomical Union (IAU), the newly discovered features are large enough, and significant enough, to warrant the assignment of names. The Committee on Nomenclature of the

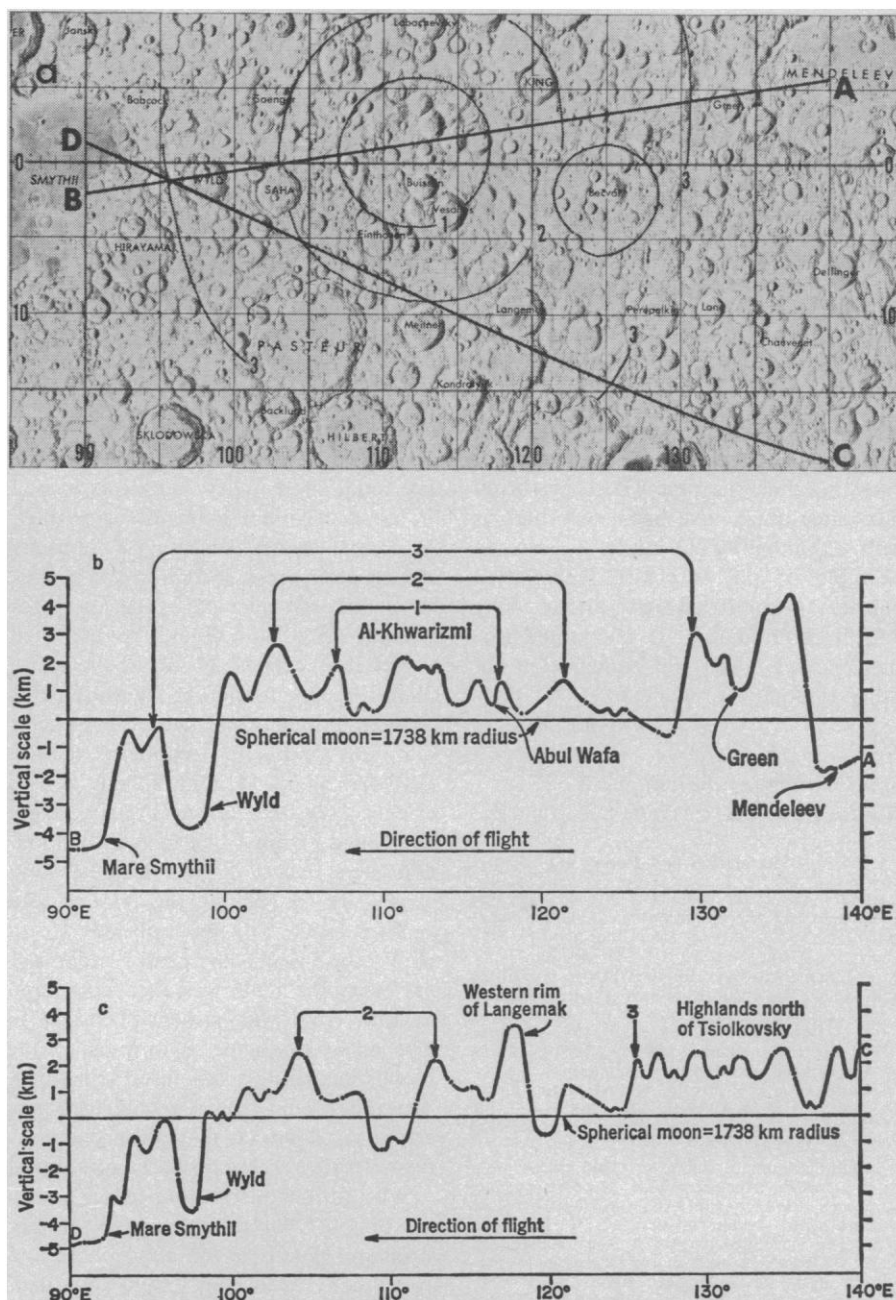


Fig. 3. (a) Traces of the laser profiles of Apollo 16 (line A-B) and Apollo 15 (line C-D), between 140°E and 90°E. The three rings of the new-found Al-Khwarizmi basin are numbered. The crater Necho, 200 km in diameter, is superposed on the eastern rim of the second ring of the basin. (b) Altitude profiles and radius deviations from the spherical moon based on Apollo 16 laser altimeter data [line A-B in (a)]. Altitude measurements were correlated with and supplemented by photography. The three rings of Al-Khwarizmi basin are numbered. (c) Altitude profiles and radius deviations from the spherical moon based on Apollo 15 laser altimeter data [line C-D in (a)]. Altitude measurements were correlated with and supplemented by photography. The profile crosses the second ring of the basin at two points and the probable third ring at about 125°E.

IAU has accepted my recommendation of the following names:

*Al-Khwarizmi*: name for the new-found basin that is centered at 1°N, 112°E (5). The name is that of the Arab scholar (approximately A.D. 780–850) who compiled the oldest astronomical tables and composed the oldest work on arithmetic. He coined the term algebra and his own name, twisted by Western tongues as algorism, denotes the system of numerals in wide use today.

*Necho*: name for the new-found, 200-km crater that is centered at 3°S, 125°E. The name is that of the ancient Egyptian pharaoh and pioneer geographer (ruled from 609 to 593 B.C.) who commissioned a successful 3-year naval expedition to prove that Africa was surrounded by water on all sides.

Discovery of these features adds another dimension to our understanding of the lunar farside highlands and crater formation in the first half billion years of the moon's history. The process of basin-filling and subsequent cratering during a time when meteoroid flux rates must have been very high is well exhibited. This study is also an example of the successful correlation between Apollo orbital photography and laser altimetry. It encourages further correlations and integration of other remotely sensed data.

FAROUK EL-BAZ

*National Air and Space Museum,  
Smithsonian Institution,  
Washington, D.C. 20560*

#### References and Notes

1. Before the crater King (5.5°N, 120.5°E) was named by the International Astronomical Union (IAU), it was given the number 211: see F. El-Baz, *Science* 167, 49 (1970).
  2. The name "Soviet Mountains" was coined by Russian investigators following interpretations of the Luna 3 photographs [N. P. Barabashov, A. A. Mikhailov, Y. N. Lipsky, *Atlas Obratnoy Storony Luny* (Nauka, Moscow, 1960)]. It was later argued that what was interpreted as a mountain range are in reality bright ejecta and rays [E. A. Whitaker, *NASA SP-201* (1969), pp. 9–12]. The name was finally rejected by the IAU in 1970.
  3. Additional photographs of the crater were obtained on Apollo mission 14, for example, frames 10298 through 10301 (also by the metric camera on Apollo mission 17, for example, frames 3183 through 3207). The relative age of the crater as well as the stratigraphic position of the basin are dealt with in D. E. Wilhelms and F. El-Baz, "Geological Map of the Eastern Limb Region of the Moon" (U.S. Geological Survey, Washington, D.C., in press).
  4. W. R. Wollenhaupt and W. L. Sjogren, *Moon* 4, 337 (1972); W. L. Sjogren and W. R. Wollenhaupt, *Science* 179, 275 (1973).
  5. The name "Arabia" was used to designate the basin during the Apollo 17 mission and also in the "Apollo 16 Preliminary Science Report" (National Aeronautics and Space Administration, Washington, D.C., 1973). Since the IAU does not encourage geographical names, the name "Arabia" was dropped in favor of "Al-Khwarizmi."
- 5 October 1972; revised 7 February 1973

## Remote Radar Sensing: Atmospheric Structure and Insects

**Abstract.** *A high-resolution radar sounder has been used in the simultaneous detection of atmospheric structure and insects. The vertical distribution of insects was often correlated with atmospheric structure. Continuous recordings revealed diurnal fluctuations and layering of insects at various altitudes.*

Research efforts in fields as diversified as air pollution, anomalous radio propagation, microphysical cloud structure, and clear air turbulence have produced a variety of active remote sensing techniques based on radar principles with the use of radio, optical, and acoustic waves (1). One of these remote sensors is a frequency-modulated, continuous-wave (FM-CW) radar, of which the most outstanding feature is the ability to observe extremely weak targets with ultrahigh range resolution at close ranges. Its sensitivity is sufficient to detect weak clear air atmospheric scattering layers and to observe structural details with a range resolution of only 1 m. A by-product of such a sensitivity is the ability to observe individual insects at large distances. The radar's sensitivity may be expressed in terms of insect detection capability. A typical insect such as a housefly (backscatter cross section =  $10^{-3}$  cm<sup>2</sup> for a radio wavelength of 10 cm) at a distance of 1 km would be expected to produce echoes 24 db above noise level. We made actual measurements of the radar echoes of two insect species (2). An individual cabbage looper, *Trichoplusia ni* (Hübner), and a field cricket, *Gryllus* (*Acheta*) sp., were suspended from a tethered balloon. One steel ball of known diameter was placed 10 m below the insect, and another steel ball was placed 10 m above the insect. The return radar signal from the balls was then compared to that from the suspended insect to give an approximate calibration of the signals returning from insects in flight. The radar echo from the cabbage looper appeared similar to typical insect returns from our atmospheric soundings.

We utilized this remote sensor's ability to observe simultaneously microstructural details in the atmosphere and insect activity at San Diego and near the southwestern shore of the Salton Sea in southern California. San Diego has a mild coastal climate, and the Salton Sea is an arid desert valley. Large areas to the north and south of the Salton Sea are irrigated farmland and serve as a breeding area for numerous insect species; most of the surrounding land area is sandy desert. A mobile FM-CW radar sounder devel-

oped at the Naval Electronics Laboratory Center in San Diego (3) was operated continuously from 28 to 31 August 1972 at the U.S. Navy Salton Sea Base south of Salton City. Of particular interest to us were the ways in which the populations of cabbage loopers and field crickets interact with atmospheric structure and with winds.

During the measurement period, the antennas were fixed vertically and continuous time-height recordings of radar echoes were obtained. Figure 1 is a 10-minute record showing an excellent example of atmospheric motion influencing insect flight patterns. A clear air atmospheric scattering layer was carried over the radar starting at 2109 P.S.T. The echo changed height from 50 m to 400 m above ground in a 3-minute period. The vertical motion associated with this echo structure influenced the paths of the insects in the vicinity. A point target, like an insect, crossing the radar beam will appear on the radar record with a sloping trace on the recording if it changes height while in the beam. Through the entire height window of the recording the slope of the insect echoes paralleled the slope of the atmospheric echo. Thus, in the absence of atmospheric echoes, insect flight patterns are possible tracers of atmospheric motion (4). The interaction of atmospheric motion and insect flight is an important unknown factor in studies of insect dispersal and migration. Insect-control programs based on such concepts as the sterile male technique and pheromone mating interruption require a reasonable estimate of potential and actual insect ranges. The ranges may depend on how insects utilize existing winds to conserve their energy or how atmospheric motion prevents insects from reaching certain locations.

Figure 1 indicates the interaction of insects and atmospheric motion, although there is no evidence that the insects actively sought this kind of interaction. In contrast, Fig. 2 shows striking examples of insects occurring at specific altitudes (radar records taken at San Diego, California). The radar record of 16 April 1972 (Fig. 2A) shows a high density of insects above an undulating atmospheric echo layer asso-